Physics-based output-feedback consensus-formation control of networked autonomous vehicles

Antonio Loria, Emmanuel Nuño, Elena Panteley, Esteban Restrepo

Publication data: chapter in *Hybrid and Networked Dynamical Systems.* Lecture Notes in Control and Information Sciences, R. Postoyan, P. Frasca, E. Panteley, L. Zaccarian, eds., London.: Springer Verlag, 2023. ISBN Hardcover: 978-3-031-49554-0 e-book: 978-3-031-495557.

Physics-based output-feedback consensus-formation control of networked autonomous vehicles

Antonio Loría*, Emmanuel Nuño†, Elena Panteley*, Esteban Restrepo‡

Abstract We describe a control method for multi-agent vehicles, to make them adopt a formation around a non pre-specified point on the plane, and with common but non pre-imposed orientation. The problem may be considered as part of a more complex maneuver in which the robots are summoned to a rendezvous to advance in formation. The novelty and most appealing feature of our control method is that it is physics-based; it relies on the design of distributed dynamic controllers that may be assimilated to second-order mechanical systems. The consensus task is achieved by making the controllers, not the vehicles themselves directly, achieve consensus. Then, the vehicles are steered into a formation by virtue of fictitious mechanical couplings with their respective controllers. We cover different settings of increasing technical difficulty, from consensus formation control of second-order integrators to second-order nonholonomic vehicles and in scenarii including both state- and output-feedback control. In addition, we address the realistic case in which the vehicles communicate over a common WiFi network that introduces time-varying delays. Remarkably, the same physics-based method applies to all the scenarii.

1 Introduction

For first and second-order integrators the leaderless consensus problem, which consists in the state variables of all agents converging to a common value, is well-studied and solved under many different scenarios [52]. However, the solution to this problem is more complex if one considers the agents' dynamics [26, 48], network constraints, such as communication delays [64], unavailability of velocity measurements [41], or nonholonomic constraints that restrict the systems' motion [28].

*Lab des signaux et systèmes, CNRS, Gif-sur-Yvette, France e-mail: antonio.loria@cnrs.fr, elena.panteley@cnrs.fr · †Department of Computer Science at the University of Guadalajara. Guadalajara, Mexico e-mail: emmanuel.nuno@academicos.udg.mx · ‡CNRS, Univ Rennes, Inria, IRISA, Campus de Beaulieu, 35042 Rennes, France e-mail: esteban.restrepo@inria.fr.

For autonomous vehicles, which, in contrast to mathematical *models* consisting of first and second-order integrators, do occupy a physical space, the leaderless consensus problem consists in making all robots converge to a *rendezvous* point. That is, the robots are required to coordinate their motions without any pre-established trajectory. Furthermore, because the robots can obviously not occupy the same physical space simultaneously, a formation pattern with an unknown center must be imposed. This is done by specifying for each robot, an offset position from the unknown center [43]. It may be required that positions and orientations converge to a common value [33], or that either only the positions [28] or only the orientations [36] achieve a common equilibrium point.

Rendezvous control is useful in cases where a group of robots must converge to postures that form a desired geometric pattern given any initial configuration in order to subsequently maneuver as a whole [63]. This is a typical two-stage formation problem. In the first, a rendezvous algorithm is required for the stabilization of the agents [21, 11, 55] and in the second a formation-tracking controller is employed [10]–[35].

From a systems viewpoint, rendezvous control of nonholonomic vehicles is inherently a set-point stabilization problem. In that regard, it presents the same technical difficulties as the stabilization of a single robot. In particular, that nonholonomic systems are not stabilizable via time-invariant smooth feedback [6], but either via discontinuous time-invariant control [11] or time-varying smooth feedback [62, 22]. In other words, in contrast to the case of holonomic systems, for systems with nonholonomic constraints stabilization is not a particular case of trajectory tracking, so controllers that solve one problem *generally* cannot solve the other [29]. For multi-agent systems, necessary conditions for rendezvous are laid in [28]. Thus, neither the numerous algorithms for consensus of linear systems nor those for formation-tracking control, notably in a leader-follower configuration, apply to the rendezvous problem for nonholonomic vehicles.

Here we consider a rendezvous problem for second-order (force-controlled) nonholonomic systems interconnected over an undirected static graph and with time-varying measurement delays for which velocity measurements are not available. From a systems viewpoint, this is an output-feedback control problem, with output corresponding to the vehicles' positions and orientations. We emphasize that in spite of the many articles on output-feedback control for the consensus of multi-agent systems—see *e.g.,* [14, 34, 61, 27], very few address the problem of output-feedback control for nonholonomic vehicles; see for instance, [50] on the leader-follower consensus problem and [18] where a velocity filter has been employed to obviate the need of velocity measurements. In the latter, however, delays are not considered and, more importantly, such problem appears to be unsolvable using the algorithm proposed therein.

In this chapter we explore the consensus-formation control problem for nonholonomic systems under various scenarii. We start by revisiting the consensus control of second-order integrators, and then we show how output-feedback consensus control may be achieved via dynamic feedback, even in the presence of transmission delays.

Our controllers are completely distributed because they rely only on the information available to each agent from its neighbors, without requiring any knowledge of the complete network.

Some of the statements presented here are original and others appear in [44] and [45]. In contrast to the latter, however, in this chapter we favor a pedagogical over a technical presentation. Hence, we omit proofs and rather develop in detail the most interesting fact that the stabilization mechanism behind our methods has a clear physical analogy with the stabilization of (under-actuated) flexible joint robots. In the following section we describe the dynamic model of the nonholonomic agents and we present the formal problem statement. Then, in Section 3 we revisit the rendezvous problem for linear second-order systems via a state-feedback controller. In Section 4 we design an output-feedback scheme for nonholonomic vehicles for the undelayed case. In Section 5 we see how our method applies even in the presence of measurement delays. In Section 6 we illustrate our findings with a case-study of realistic simulations, for which we used the Gazebo-ROS environment. As customary, we offer some concluding remarks in Section.

2 Model and problem formulation

2.1 Single-robot model

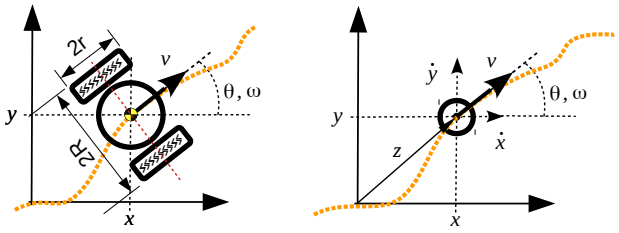

Fig. 1 Schematics of a differential-drive mobile robot

We consider autonomous vehicles as the one schematically represented in Figure 1. Its position on the plane may be defined as that of its center of mass, with Cartesian coordinates $(x, y) \in \mathbb{R}^2$ and its orientation with respect to the abscissae is denoted by the angle θ. It is assumed that the vehicle may move forward with a velocity $v := [\dot{x}^2 + \dot{y}^2]^{(1/2)}$ and turn with an angular velocity ω. The vehicle, however, cannot move in certain directions (*e.g.,* sideways). This restriction is encoded by the non-integrable velocity constraint

$$\sin(\theta)\dot{x} = \cos(\theta)\dot{y}.$$

From these expressions we obtain the velocity equations

$$\dot{x} = \cos(\theta)v \tag{1a}$$
$$\dot{y} = \sin(\theta)v \tag{1b}$$
$$\dot{\theta} = \omega, \tag{1c}$$

which define a *first-order* model often used in the literature on control of nonholonomic systems —see *e.g.,* [10, 37, 40, 60] and [35]. In such model the control inputs are the velocities v and ω. Being mechanical systems, however, a more complete model includes a set of Euler-Lagrange equations for the velocity dynamics, *i.e.,*

$$\dot{v} = F_v(z, \theta, v, \omega) + u_v \tag{2a}$$
$$\dot{\omega} = F_\omega(z, \theta, v, \omega) + u_\omega, \tag{2b}$$

where F_v and F_ω are smooth functions [39]. Articles on *control* of nonholonomic systems where such *second-order* models are used are considerably scarce in comparison —see, *e.g.,* see [9] and [15] and they are more often found in a single-vehicle setting [24, 13, 19].

Here, we employ a complete second-order model that corresponds to that of so-called differential-drive robots [59]. For the purpose of analysis, only, we assume that the center of mass is aligned with an axis joining the centers of the wheels—see the illustration on the left in Figure 1, so $F_\omega = F_v \equiv 0$, but the model used to test our algorithms in the realistic simulator Gazebo-ROS does not satisfy this assumption.

Thus, the control inputs take the form

$$u_v := \frac{1}{rm}[\tau_1 + \tau_2], \quad u_\omega := \frac{2R}{Ir}[\tau_1 - \tau_2],$$

where m and I are respectively the robot's mass and inertia whereas τ_1 and τ_2 are the torques applied, independently, at each of the wheels.

An essential feature of this model, that is at the basis of the control design, is that Equations (1)–(2) consist of *two* coupled second-order systems driven by independent control inputs. One system determines the linear motion and the other the angular one. To evidence this, we define $z_i := [x_i \; y_i]^\top \in \mathbb{R}^2$, where we introduced the index $i \leq N$ to refer to one among N robots —see the illustration on the right in Figure 1, and rewrite the equations for the ith robot in the form:

$$\text{angular-motion dynamics} \begin{cases} \dot{\theta}_i = \omega_i & \text{(3a)} \\ \dot{\omega}_i = u_{\omega i}, & \text{(3b)} \end{cases}$$

$$\text{linear-motion dynamics} \begin{cases} \dot{z}_i = \varphi(\theta_i)v_i, & \text{(4a)} \\ \dot{v}_i = u_{vi}, & \text{(4b)} \end{cases}$$

where

$$\varphi(\theta_i) := [\cos(\theta_i) \quad \sin(\theta_i)]^\top. \tag{5}$$

This (apparently innocuous) observation is important because the literature is rife with efficient controllers for second-order mechanical systems from which we may draw inspiration for the problem at hand here, even in the context of multi-agent systems [52]. Moreover, even though the subsystems (3) and (4) are clearly entangled through the function φ they may be dealt with as if decoupled, by replacing θ_i with the trajectory $\theta_i(t)$ since φ is uniformly bounded [30]. Hence, relying on a cascades argument, we may apply a separation principle to design the controllers for the linear and angular motion subsystems independently. These key features are at the basis of our method to approach the rendezvous problem, which is described next.

2.2 The consensus formation problem

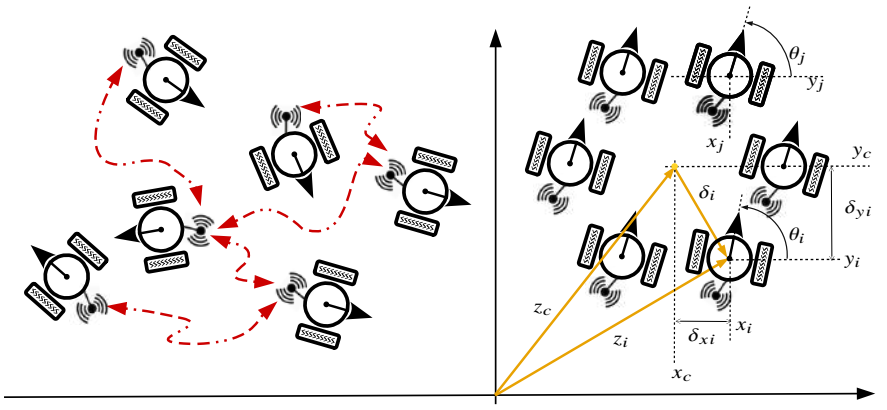

Fig. 2 Vehicles initially dispersed communicating over an undirected network (are required to) achieve formation consensus around a rendezvous point

Consider a group of N force-controlled nonholonomic vehicles modeled by (3)–(5) like the one depicted in Figure 1, each of these robots is assumed to be equipped with positioning sensors that deliver reliable measures of x_i, y_i, and θ_i.

The robots are required to meet in formation at a rendezvous point $z_c := (x_c, y_c)$ and acquire a common orientation θ_c. That is, for each $i \leq N$ the Cartesian positions z_i must converge to $z_c + \delta_i$, where δ_i is a vector that determines the position of the ith vehicle relative to the unknown center of the formation —see Figure 2 for an illustration. More precisely, consider the following problem statement.

Definition 1 (Consensus formation) For each robot (resp. each $i \leq N$), given a vector $\delta_i = [\delta_{xi}\ \delta_{yi}]^\top$, define its translated position $\bar{z}_i := z_i - \delta_i$ (correspondingly, let $\bar{x}_i := x_i - \delta_{xi}$ and $\bar{y}_i := y_i - \delta_{yi}$).

Then, design a distributed controller such that

$$\lim_{t\to\infty} v_i(t) = 0, \quad \lim_{t\to\infty} \bar{z}_i(t) = z_c, \tag{6}$$

$$\lim_{t\to\infty} \omega_i(t) = 0, \quad \lim_{t\to\infty} \theta_i(t) = \theta_c \qquad \forall\, i \leq N. \tag{7}$$

We stress that this is a leaderless consensus problem. That is, neither the coordinates (x_c, y_c) nor the angle θ_c are determined a priori as a reference. They depend on the initial postures, the systems' nonlinear dynamics, and network features (see farther below). In general, this problem, may not be solved using controllers designed to make the vehicles advance in formation while following a leader (virtual or otherwise).

Now, we assume that the vehicles communicate over a WiFi network. The ith robot communicates with a set of neighbors, which we denote by $\mathcal{N}_i$. It is naturally assumed that once a communication is set between two robots i and $j \in \mathcal{N}_i$, the flow of information is bidirectional and is never lost. More precisely, we pose the following.

Assumption 1 *The network may be modeled using an interconnection graph that is undirected, static, and connected.*

Remark 1 In graph theory, a graph is undirected if the nodes exchange information in both directions, it is static if the interconnection is constant, and an undirected graph is connected if any node is reachable from any other node.

Now, because the robots communicate over a WiFi network, the communication between the robots i and j is affected by non-constant time-delays. More precisely, we consider the following.

Assumption 2 *The communication from the jth to the ith robot is subject to a variable time-delay denoted $T_{ji}(t)$ that is bounded by a known upper-bound $\overline{T}_{ji} \geq 0$ and has bounded time-derivatives, up to the second.*

Furthermore, we also assume that the vehicles are equipped only with position and orientation sensors. That is,

Assumption 3 *the velocities v_i and ω_i are not measurable.*

Assumptions 1–3 coin realistic scenarii of automatic control of multi-agent systems, but all three together have been little addressed in the literature in the context of consensus control of nonholonomic systems [45]. Yet, Assumption 2 carries certain conservatism in imposing that the delays be differentiable and bounded. Indeed, it must be stressed that, in general, time-delays over WiFi networks or the Internet may rather be of a non-smooth nature [1, 2, 33]. Nonetheless, the formal analysis under such condition is considerably intricate and escapes the scope of this document. For a Lyapunov-based analysis of the rendezvous problem under non-differentiable delays, albeit via state-feedback, see [32, 33].

3 Control Architecture: state-feedback case

As previously implied, the controller that we propose relies on the system's structural properties that lead to a separation of the linear- and angular-motion dynamics. For clarity of exposition, we start by revisiting the consensus problem for ordinary second-order systems ('double integrators') via state-feedback and without delays. The purpose is to underline the robustness of a commonly used distributed controller, by presenting an original analysis that is helpful to understand the essence of the stabilization mechanism at the basis of our method. In addition, it has the advantage of providing a strict Lyapunov function for consensus of second-order systems.

3.1 Consensus control of second-order systems

The consensus problem for systems with dynamics—*cf.* Eq. (3),

$$\ddot{\vartheta}_i = u_i \quad i \leq N,\ u_i \in \mathbb{R} \tag{8}$$

(that is, steering $\vartheta_i \to \vartheta_c$, $\dot{\vartheta}_i \to 0$, and $\ddot{\vartheta}_i \to 0$ with ϑ_c constant and non-imposed *a priori*) is now well understood in various settings, *e.g.,* in the case of unmeasurable velocities [3], of measurement delays [17], or with state constraints [51, 53].

For instance, it is well known (see [52]) that if the systems modeled by (8) communicate over a network modeled by a directed, static, and connected graph, and the full state is measurable, the distributed control law of proportional-derivative (PD) type

$$u_i = -d_i\dot{\vartheta}_i - p_i \sum_{j\in\mathcal{N}_i} a_{ij}(\vartheta_i - \vartheta_j), \quad d_i,\ p_i > 0, \tag{9}$$

where $a_{ij} > 0$ if $j \in \mathcal{N}_i$ and $a_{ij} = 0$ otherwise, solves the consensus problem. More precisely, we have the following.

Proposition 1 *Consider the system* (8) *in closed loop with* (9)*, that is, the system*

$$\ddot{\vartheta}_i + d_i\dot{\vartheta}_i + p_i \sum_{j\in\mathcal{N}_i} a_{ij}(\vartheta_i - \vartheta_j) = 0. \tag{10}$$

Then, the consensus manifold $\{\vartheta_i = \vartheta_j\} \cap \{\dot{\vartheta}_i = 0\}$*, for all* $i,\ j \leq N$ *is globally exponentially stable for any positive values of* d_i *and* p_i*.*

The proof of global asymptotic stability of the consensus manifold is well reported in the literature [52]. For further development we provide here a simple and original proof of global *exponential* stability based on Lyapunov's direct method.

Let $\vartheta := [\vartheta_1 \ \cdots \ \vartheta_N]^\top$,

$$\tilde{\vartheta} := \vartheta - \frac{1}{N}\mathbf{1}_N\mathbf{1}_N^\top\vartheta, \quad \text{where} \quad \mathbf{1}_N := [1 \cdots 1]^\top. \tag{11}$$

The ith element of the vector $\tilde{\vartheta}$ denotes the difference between ϑ_i and the average of all the states, *i.e.,* $\vartheta_c := (1/N)\mathbf{1}_N^\top \vartheta$, so consensus is reached if and only if $\tilde{\vartheta} = 0$. In addition, under Assumption 1, ϑ_c corresponds to the consensus equilibrium point. Now, to abbreviate the notation, we also define

$$R := I - \frac{1}{N}\mathbf{1}_N\mathbf{1}_N^\top.$$

Note that $R = R^\top$ and $\|R\| \leq 1$, where $\|R\|$ corresponds to the induced norm of R, and $\tilde{\vartheta} = R\vartheta$.

Next, we introduce the Laplacian matrix, $L := [\ell_{ij}] \in \mathbb{R}^{N\times N}$, where

$$\ell_{ij} = \begin{cases} \sum\limits_{k\in\mathcal{N}_i} a_{ik} & i = j \\ -a_{ij} & i \neq j. \end{cases} \tag{12}$$

By construction, $L\mathbf{1}_N = 0$ and, after Assumption 1, L is symmetric, it has a unique zero-eigenvalue, and all of its other eigenvalues are strictly positive. Hence, $\text{rank}(L) = N - 1$. Also, the last term on the right-hand side of Equation (9) satisfies

$$\text{col}\Big[\sum_{j\in\mathcal{N}_i} a_{ij}(\vartheta_i - \vartheta_j)\Big] = L\tilde{\vartheta}, \tag{13}$$

where $\text{col}[(\cdot)_i]$ denotes a column vector of N elements $(\cdot)_i$. Indeed, by the definition of the Laplacian, we have

$$\text{col}\Big[\sum_{j\in\mathcal{N}_i} a_{ij}(\vartheta_i - \vartheta_j)\Big] = L\Big[\vartheta - \frac{1}{N}\mathbf{1}_N\mathbf{1}_N^\top\vartheta\Big] + \frac{1}{N}L\mathbf{1}_N\mathbf{1}_N^\top\vartheta.$$

However, $L\mathbf{1}_N = 0$, so the right hand side of the equation above equals to $LR\vartheta$, which corresponds to $L\tilde{\vartheta}$, by definition. These identities are useful to write the closed-loop system (8)–(9) in the multi-variable form

$$\ddot{\vartheta} = -D\dot{\vartheta} - PL\tilde{\vartheta}, \tag{14}$$

where $P := \text{diag}[p_i]$ and $D := \text{diag}[d_i]$. In turn, this serves to notice that the Lyapunov function

$$V_1(\tilde{\vartheta}, \dot{\vartheta}) := \frac{1}{2}\Big[\tilde{\vartheta}^\top L\tilde{\vartheta} + \dot{\vartheta}^\top P^{-1}\dot{\vartheta}\Big] \tag{15}$$

is positive definite, even if L is rank deficient. Indeed, the term $\tilde{\vartheta}^\top L\tilde{\vartheta} \geq \lambda_2(L)|\tilde{\vartheta}|^2$, where $\lambda_2(L) > 0$ corresponds to the second eigenvalue of L (that is, the smallest positive eigenvalue). We stress that V_1 is positive, not for *any* $\tilde{\vartheta} \in \mathbb{R}^N\backslash\{0\}$, but for $\tilde{\vartheta}$ as defined in (11).

Now, evaluating the total derivative of V_1 along the trajectories of (14) and using $L\dot{\tilde{\vartheta}} = L\dot{\vartheta}$ (again, this holds because $L\mathbf{1}_N = 0$) we see that

$$\dot{V}_1(\tilde{\vartheta}, \dot{\vartheta}) = -\dot{\vartheta}^\top P^{-1}D\,\dot{\vartheta}. \tag{16}$$

Global asymptotic stability of the consensus manifold $\{(\tilde{\vartheta}, \dot{\vartheta}) = (0, 0)\}$ may be ascertained from (16) by invoking Barbashin-Krasovskĭi's theorem [4] (also, but wrongly, known as LaSalle's theorem).

Remark 2 Note that, in the presence of an additional input α the system (14), that is, $\ddot{\vartheta} + D\dot{\vartheta} + PL\tilde{\vartheta} = \alpha$, defines an output strictly passive map $\alpha \mapsto \dot{\vartheta}$. This follows by a direct computation of $\dot{V}_1$ that leads to $\dot{V}_1(\tilde{\vartheta}, \dot{\vartheta}) = -\dot{\vartheta}^\top P^{-1} D\, \dot{\vartheta} + \alpha^\top \dot{\vartheta}$.

As a matter of fact, since the system is linear time-invariant, it is also globally exponentially stable. To see this more clearly, using V_1 it is possible to construct a simple strict Lyapunov function. This is useful to assess the robustness of system (8) in closed loop with the consensus control law defined in (9) in terms of input-to-state stability.

Let $\varepsilon \in (0, 1)$ and define

$$V_2(\tilde{\vartheta}, \dot{\vartheta}) := V_1(\tilde{\vartheta}, \dot{\vartheta}) + \varepsilon \tilde{\vartheta}^\top P^{-1} \dot{\vartheta}. \tag{17}$$

In view of the properties of V_1 it is clear that also V_2 is positive definite and radially unbounded, for sufficiently small values of ε. On the other hand, the total derivative of V_2 along the closed-loop trajectories of (14) yields

$$\dot{V}_2(\tilde{\vartheta}, \dot{\vartheta}) = \dot{V}_1 + \varepsilon \Big[\dot{\vartheta}^\top R P^{-1} \dot{\vartheta} - \tilde{\vartheta}^\top P^{-1} D \dot{\vartheta} - \tilde{\vartheta}^\top L \tilde{\vartheta} \Big], \tag{18}$$

which, in view of (16) and the fact that $\|R\| \leq 1$, implies that

$$\dot{V}_2(\tilde{\vartheta}, \dot{\vartheta}) \leq -c_1 |\dot{\vartheta}|^2 - \varepsilon c_2 |\tilde{\vartheta}|^2 \tag{19}$$

where d_m and p_M are the smallest and largest coefficients of D and P respectively, $c_1 := \frac{d_m}{p_M} - \varepsilon \big[\frac{1}{p_m} + \frac{d_M}{2\lambda p_m} \big]$ and $c_2 := \ell_2 - \frac{\lambda}{2} \frac{d_M}{p_m}$ are positive for appropriate values of λ and $\varepsilon \in (0, 1)$ and any $\ell_2 := \lambda_2(L) > 0$.

The previous analysis is interesting because it leads to the important observation that for perturbed systems with dynamics $\ddot{\vartheta}_i = u_i + \alpha_i$ where α_i is a bounded external disturbance, we have

$$\dot{V}_2(\tilde{\vartheta}, \dot{\vartheta}) \leq -c_1' |\dot{\vartheta}|^2 - \varepsilon c_2' |\tilde{\vartheta}|^2 + c_3 |\alpha|^2 \tag{20}$$

where $c_1' := c_1 - \frac{\lambda}{2}$, $c_2' := c_2 - \frac{d_m}{2\lambda p_m}$, and $\alpha := [\alpha_1 \cdots \alpha_N]^\top$. So the closed-loop system is input-to-state stable with respect to the input α.

We use the previously established facts in our control-design method. The controllers that we present below, for nonholonomic systems, are devised as second-order mechanical systems in closed loop with a consensus controller, that is, with dynamics reminiscent of (14). Then, they are interconnected via virtual springs to the vehicles' dynamics so that, by virtue of reaching consensus among themselves, they stir the vehicles to consensus too.

Thus, following, on one hand, the previous developments for consensus of second-order integrators and, on the other, the fact that the nonholonomic vehicle's dynamics consist mainly in two interconnected second-order mechanical systems, we proceed

to design a consensus-formation controller for nonholonomic systems. The input-to-state stability property previously underlined is fundamental to devise the controllers separately, for the linear- and angular-motion dynamics.

3.2 State-feedback consensus control of nonholonomic vehicles

We start our control design with the angular-motion dynamics (3), which we rewrite in the form $\ddot{\theta}_i = u_{\omega i}$ for convenience—*cf.* (8). Then, we introduce the control law

$$u_{\omega i} = -d_{\omega i}\dot{\theta}_i - p_i \sum_{j\in\mathcal{N}_i} a_{ij}(\theta_i - \theta_j) \quad d_{\omega i},\ p_{\omega i} > 0, \tag{21}$$

which is the same as (9), up to an obvious change in the notation. Hence, the closed-loop system (3)–(21) yields

$$\ddot{\theta}_i + d_{\omega i}\dot{\theta}_i + p_i \sum_{j\in\mathcal{N}_i} a_{ij}(\theta_i - \theta_j) = 0. \tag{22}$$

From Proposition 1 it follows that the consensus manifold $\{\omega_i = 0\} \cap \{\theta_i = \theta_j\}$ is globally exponentially stable for (22). Therefore, $\theta_i \to \theta_c$ for all $i \leq N$.

It is left to design a consensus controller of the form (9) for the linear-motion dynamics (4). In this case, however, the consensus error feedback must take into account the kinematics function φ. That is, we pose the control law—cf. [5]. Let

$$u_{vi} = -d_{vi}v_i - p_{vi}\varphi(\theta_i)^\top \sum_{j\in\mathcal{N}_i} a_{ij}(\bar{z}_i - \bar{z}_j). \tag{23}$$

Then, for the purpose of analysis we replace the state variable θ_i with an arbitrary trajectory $\theta_i(t)$. This is possible because $t \mapsto \theta_i(t)$, as a solution of (22), exists on $[0, \infty)$ and so does its first derivative, that is, $t \mapsto \omega_i(t)$. Hence,the closed-loop linear-motion dynamics (4)-(23) may be regarded as a *time-varying* subsystem[1], decoupled from the angular motion dynamics. That is,

$$\Sigma_{vi} : \begin{cases} \dot{\bar{z}}_i = \varphi(\theta_i(t))v_i, & \text{(24a)} \\ \dot{v}_i = -d_{vi}v_i - p_{vi}\varphi(\theta_i(t))^\top \sum_{j\in\mathcal{N}_i} a_{ij}(\bar{z}_i - \bar{z}_j). & \text{(24b)} \end{cases}$$

Then, to analyze the stability of the consensus manifold for (24), akin to V_1 in (15), we define the Lyapunov function

$$V_3(v, \bar{z}) := \frac{1}{2}\sum_{i\leq N}\Big[\frac{1}{p_{vi}}v_i^2 + \frac{1}{2}\sum_{j\in\mathcal{N}_i} a_{ij}|\bar{z}_i - \bar{z}_j|^2\Big], \tag{25}$$

where $v := [v_1\ \cdots\ v_N]^\top$ and $\bar{z} := [\bar{z}_1\ \cdots\ \bar{z}_N]^\top$ —cf. (13).

[1] To prove further see [23, p. 657] and [30].

Using the identity

$$\frac{1}{2}\sum_{i\leq N}\sum_{j\in\mathcal{N}_i} a_{ij}(\dot{\bar{z}}_i-\dot{\bar{z}}_j)^\top(\bar{z}_i-\bar{z}_j)=\sum_{i\leq N} a_{ij}\dot{\bar{z}}_i^\top(\bar{z}_i-\bar{z}_j)$$

—see [46] and [8, Lemma 6.1], we compute the total derivative of V_3 along the closed-loop trajectories of (24). We obtain

$$\dot{V}_3(v,\bar{z})=-v^\top D_v P_v^{-1} v, \tag{26}$$

where $P_v := \mathrm{diag}[p_{vi}]$ and $D_v := \mathrm{diag}[d_{vi}]$.

Now, the system in (24) being non-autonomous, Barbashin-Krasovskĭi's theorem does not apply, but we may use Barbălat's [23] to assess global asymptotic stability. To that end, we first remark that the function V_3 is positive definite and radially unbounded in v_i and $|\bar{z}_i-\bar{z}_j|$ for all $i, j \leq N$. Then, integrating along the trajectories on both sides of the identity (26) and of the inequality $\dot{V}_3(v(t),\bar{z}(t))\leq 0$, we obtain that v_i and $|\bar{z}_i-\bar{z}_j|$ are bounded, *i.e.*, $v_i, |\bar{z}_i-\bar{z}_j|\in\mathcal{L}_\infty$ and $v_i\in\mathcal{L}_2$. In addition, (26) implies that the consensus equilibrium defined by $\{v_i=0,\ \bar{z}_i=\bar{z}_j\}$ is stable. From (24), the boundedness and continuity of $\varphi(\theta_i)$, of $\theta_i(t)$, and of $\omega_i(t)=\dot{\theta}_i(t)$, we see that, also, $\dot{\bar{z}}_i$, $\dot{v}_i$, and, consequently, $\ddot{v}_i\in\mathcal{L}_\infty$. Since $v_i\in\mathcal{L}_2\cap\mathcal{L}_\infty$ and $v_i\in\mathcal{L}_\infty$ we conclude that $v_i\to 0$. Hence, since

$$\lim_{t\to\infty}\int_0^t \dot{v}_i(s)ds=\lim_{t\to\infty} v_i(t)-v_i(0),$$

we have

$$\lim_{t\to\infty}\int_0^t \dot{v}_i(s)ds=-v_i(0).$$

That is, the limit of $\dot{v}_i$ "exists and is finite" whereas the boundedness of $\ddot{v}_i$ implies that $\dot{v}_i$ is uniformly continuous. Hence, by virtue of Barbălat's Lemma, we conclude that $\dot{v}_i\to 0$ as well. In turn, after (24) we see that

$$\lim_{t\to\infty}\varphi(\theta_i(t))^\top\sum_{j\in\mathcal{N}_i} a_{ij}\big(\,\bar{z}_i(t)-\bar{z}_j(t)\,\big)=0.$$

This expression, however, does not imply that the consensus objective is reached. Indeed, note that the set of equilibria of the system in (24) corresponds to points belonging to the set

$$\mathcal{U}:=\Big\{\,v_i=0\quad\wedge\quad\varphi(\theta_i)^\top\sum_{j\in\mathcal{N}_i} a_{ij}(\bar{z}_i-\bar{z}_j)=0\,\Big\}, \tag{27}$$

which admits points such that $\bar{z}_i\neq\bar{z}_j\in\mathbb{R}^2$ because $\mathrm{rank}\,\varphi(\theta_i)=1$. This means that if orientation consensus is reached and, for instance, $\theta_i(t)\to 0$ then $\bar{x}_i\to x_c$, but $\bar{y}_i\not\to y_c$ —see Eq. (5).

Remark 3 This shows that the consensus problem for nonholonomic systems cannot be treated as that for ordinary second-order systems like those discussed in Section 3.1 —cf. [51, 20].

To ensure consensus it is necessary that the set of equilibria correspond to the set $\mathcal{U} \cap \mathcal{U}^{\perp}$, where

$$\mathcal{U}^{\perp} := \Big\{ v_i = 0 \quad \wedge \quad \varphi(\theta_i)^{\perp\top} \sum_{j \in \mathcal{N}_i} a_{ij}(\bar{z}_i - \bar{z}_j) = 0 \Big\},$$

and

$$\varphi(\theta_i)^{\perp} := [-\sin(\theta_i) \quad \cos(\theta_i)]^{\top}. \tag{28}$$

That is, $\varphi(\theta_i)^{\perp}$ is the annihilator of $\varphi(\theta_i)$ hence, $\varphi(\theta_i)^{\perp\top}\varphi(\theta_i) = \varphi(\theta_i)^{\top}\varphi(\theta_i)^{\perp} = 0$.

Roughly speaking, the controller must "pull" out the trajectories that may eventually get "trapped" in the set $\mathcal{U}$, whereas they do not belong to the set $\mathcal{U}^{\perp}$. To that end, we endow the angular-motion controller with a term that incorporates an external function of time (smooth and bounded) and acts as a perturbation to the angular-motion closed-loop dynamics. This perturbation is designed to *persist* as long as

$$\varphi(\theta_i(t))^{\perp\top} \sum_{j \in \mathcal{N}_i} a_{ij}\big(\bar{z}_i(t) - \bar{z}_j(t)\big) \neq 0. \tag{29}$$

More precisely, let ψ_i, $\dot{\psi}_i$, and $\ddot{\psi}_i$ be bounded (belong to $\mathcal{L}_\infty$) let $\dot{\psi}_i$ be persistently exciting [38], that is, let there exist T and $\mu > 0$ such that

$$\int_t^{t+T} \dot{\psi}_i(s)^2 ds \geq \mu \quad \forall\, t \geq 0. \tag{30}$$

Thus, we endow the control law in (21) with the additional term

$$\alpha_i(t, \theta_i, \bar{z}_i) := k_{\alpha i}\psi_i(t)\varphi_i(\theta_i)^{\perp\top}(\bar{z}_i - \bar{z}_j), \quad k_{\alpha i} > 0, \tag{31}$$

that is, we redefine the control law (21) as

$$u_{\omega i} = -d_{\omega i}\dot{\theta}_i - p_i \sum_{j \in \mathcal{N}_i} a_{ij}(\theta_i - \theta_j) + \alpha_i(t, \theta_i, \bar{z}_i). \tag{32}$$

To the angular-motion dynamics, α_i acts as a bounded (see Remark 4 below), hence innocuous, perturbation on the angular-motion closed-loop dynamics

$$\Sigma_{\omega i} \ : \ \ddot{\theta}_i + d_{\omega i}\dot{\theta}_i + p_i \sum_{j \in \mathcal{N}_i} a_{ij}(\theta_i - \theta_j) = \alpha_i(t, \theta_i, \bar{z}_i) \tag{33}$$

that impedes θ_i to remain in an unwanted manifold of equilibria, as long as the position consensus has not been achieved, that is, as long as (29). That is, through $\theta(t)$ in (24), the term α_i injects excitation into the system, as long as the consensus goal remains unachieved.

Now, since the system (33) is input-to-state stable with respect to α_i, the resulting closed-loop equations consist in the "cascaded" nonlinear time-varying system formed by Σ_{vi} in (24) and (33), as illustrated by Figure 3 below.

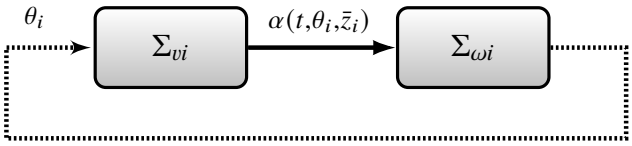

Fig. 3 Schematic representation of the closed-loop system, consisting in the error equations for the angular and the linear-motion dynamics. Even though the systems are feedback interconnected, for the purpose of analysis, they may be regarded as in cascade [30], whence the feedback of θ_i is represented by a dashed arrow.

Global asymptotic stability of the respective consensus manifolds for Σ_{vi} and $\Sigma_{\omega i}$ with $\alpha_i \equiv 0$, the input-to-state stability of (33) and a cascades argument [30] leads to the following statement—*cf.* [5, 43].

Proposition 2 *(State feedback formation consensus) Consider the system* (3)–(5) *in closed loop with* (23) *and* (32) *with* p_{vi}, d_{vi}, $p_{\omega i}$, *and* $d_{\omega i} > 0$, α_i *as in* (31), ψ_i *and* $\dot{\psi}_i$ *bounded, and* $\dot{\psi}_i$ *persistently exciting. Then, the consensus-formation goal is achieved, that is,* (6) *and* (7) *hold.*

Remark 4 (Sketch of proof of Proposition 2) Technically, the proof of this statement follows along the lines discussed above for the case in which $\alpha_i \equiv 0$. In this case, we have a cascade from $\Sigma_{\omega i}$ to Σ_{vi}. If $\alpha_i \not\equiv 0$, the cascade structure is broken, but we can still use the ISS property of (33) to *break the loop* [30].

For (33) Inequality (20) holds (up to obvious changes in the notation) for any continuous α_i. Now, let $t_f \leq \infty$ define the maximal length of the interval of existence of solutions and consider (20) along the trajectories of (33). We have

$$\dot{V}_2(\tilde{\theta}(t),\omega(t)) \leq -c_1'|\omega(t)|^2 - \varepsilon c_2'|\tilde{\theta}(t)|^2 + c_3|\alpha(t,\theta(t),\bar{z}(t))|^2 \qquad \forall\, t \in [0,t_f), \quad (34)$$

where $\tilde{\theta} := \theta - \frac{1}{N}\mathbf{1}_N\mathbf{1}_N^\top\theta$, $\theta = \mathrm{col}[\theta_i]$, and $\omega = \dot{\theta}$. On the other hand, on the interval of existence of solutions, (26) also holds along the trajectories. Thus, since $\alpha_i(t,\theta_i,\bar{z})$ is linear in $[\bar{z}_i - \bar{z}_j]$, continuous and bounded in t and θ_i, the term $|\alpha(t,\theta(t),\bar{z}(t))|^2$ remains bounded on $t \in [0,t_f)$. Moreover, there exists $c > 0$ such that $|\alpha(t,\theta,\bar{z})|^2 \leq cV_3(v,\bar{z})$. It follows from (26) and (34) that, defining $v_4(t) := V_2(\tilde{\theta}(t),\omega(t)) + V_3(v(t),\bar{z}(t))$,

$$\dot{v}_4(z(t)) \leq cv_4(t) \quad \forall\, t \in [0,t_f). \qquad (35)$$

Rearranging terms and integrating on both sides of the latter from 0 to t_f we see that

$$\int_{v_4(0)}^{v_4(t_f)} \frac{1}{cv_4} dv_4 \leq t_f.$$

That is, $\ln\left(\nu_4(t_f)/\nu_4(0)\right) \leq t_f$ (without loss of generality we assume that $\nu_4(0) > 0$). Now, since $\nu_4(t) \to \infty$ as $t \to t_f$ it follows that $t_f \not< \infty$—indeed, the postulate that $t_f < \infty$ leads to a contradiction. Therefore, the system is forward complete, (26) holds along the trajectories on $[0, \infty)$, $|\bar{z}_i(t) - \bar{z}_j(t)|$ and $v_i(t)$ are bounded on $[0, \infty)$, and so are $\tilde{\theta}(t)$ and $\omega(t)$ in view of the ISS property. On one hand, the presence of α_i prevents the solutions from remaining (close to) the set $\mathcal{U}$ in (27) and, on the other, $\alpha_i \to 0$ as the solutions converge to $\mathcal{U} \cap \mathcal{U}^{\perp}$. The result follows.

Remark 5 Controllers for nonholonomic systems that make explicit use of persistency of excitation were first used for tracking in [47] and for set-point stabilization in [31], but the underlying ideas are already present in [56, 57]. Nowadays, persistency of excitation is recognized as a fundamental, if not necessary, condition [29], for set-point stabilization of nonholonomic systems via smooth feedback and they are also frequently used in trajectory-tracking scenarii —see *e.g.,* [12, 25].

4 Control architecture: output-feedback case

In the case that velocities are unmeasurable, the velocity-feedback terms $d_{vi}v_i$ and $d_{\omega i}\omega_i$ cannot be used, so we design dynamic output-feedback controllers for the angular and linear-motion dynamics. These controllers are designed as virtual mass-spring-damper mechanical systems hinged to the vehicles' dynamics. In accordance with the separation-principle approach these controllers are designed independently for the angular and linear-motion dynamics. In addition, as before, we use persistency of excitation to overcome the difficulties imposed by the nonholonomic constraints.

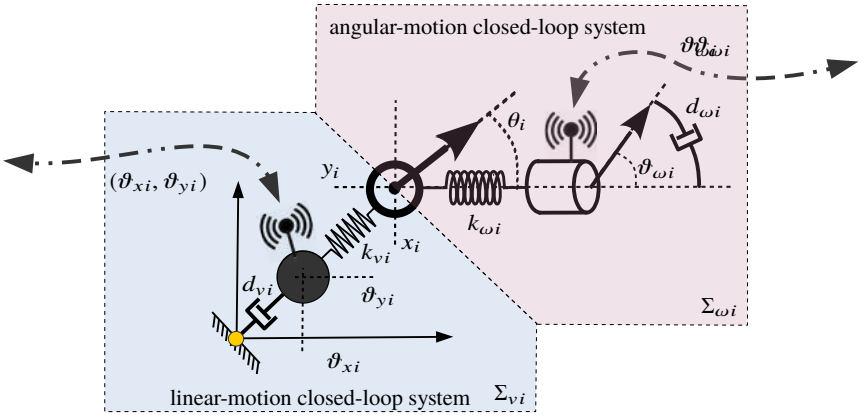

Fig. 4 Schematic representation of coupled mass-spring-damper systems: angular motion. It is the controller state variable, $\vartheta_{\omega i}$ that is transmitted to neighboring robots and, correspondingly, $\vartheta_{\omega j}$ is received from $\mathcal{N}_i$ neighbors. The system at the intersection of the two blocks represents the nonholonomic vehicle—*cf.* Figure 1.

4.1 Output-feedback orientation consensus

Expressed as $\ddot{\theta}_i = u_{\omega i}$, the angular-motion dynamics (3) corresponds to an elementary Newtonian force-balance equation with unitary inertia. The problem at hand still is to synchronize the angular positions θ_i for N such systems, but since ω_i is not available from measurement, we cannot use the control law in (21). Yet, it appears reasonable to conjecture that the objective $\theta_i \to \theta_j$ for all $i, j \leq N$ may be achieved by coupling the subsystems $\ddot{\theta}_i = u_{\omega i}$, via torsional springs, to virtual second-order oscillators, whose states are available. Then, it is the controllers' variables that are transmitted over the network to achieve consensus among the *controllers*—see Figure 4 for an illustration.

More precisely, consider the dynamic system

$$\ddot{\vartheta}_{\omega i} + d_{\omega i}\dot{\vartheta}_{\omega i} + p_{\omega i}\sum_{j\in\mathcal{N}_i} a_{ij}(\vartheta_{\omega i} - \vartheta_{\omega j}) = \nu_{\omega i} \tag{36}$$

where $\nu_{\omega i}$ is an external input to be defined, the state $\vartheta_{\omega i} \in \mathbb{R}$, and $d_{\omega i}, p_{\omega i} > 0$.

As we showed in Section 3.1, for (36) consensus is achieved, that is, there exists a real constant $\vartheta_{\omega c}$, such that $\vartheta_{\omega i} \to \vartheta_{\omega c}$, $\dot{\vartheta}_{\omega i} \to 0$, for all $i \leq N$, provided that $d_{\omega i}, p_{\omega i} > 0$, and $\nu_{\omega i} = 0$. On the other hand, the system in (36) defines a passive map $\nu_{\omega i} \mapsto \dot{\vartheta}_{\omega i}$—*cf.* Remark 2. Furthermore, the system (3b) also defines a passive map, $u_{\omega i} \mapsto \omega_i$. Therefore, it results natural to hinge the systems (36) and (3) by setting $\nu_{\omega i} := -u_{\omega i}$ and

$$u_{\omega i} := -k_{\omega i}(\theta_i - \vartheta_{\omega i}), \quad k_{\omega i} > 0. \tag{37}$$

That is, the coupling $-k_{\omega i}(\theta_i - \vartheta_{\omega i})$ may be interpreted as the force exerted by a torsional spring that hinges the (angular) positions of the two subsystems. The closed-loop system corresponding to the vehicle's angular dynamics is

$$\Sigma_{\omega i} : \begin{cases} \ddot{\theta}_i = -k_{\omega i}(\theta_i - \vartheta_{\omega i}) & \text{(38a)} \\ \ddot{\vartheta}_{\omega i} + d_{\omega i}\dot{\vartheta}_{\omega i} + p_{\omega i}\sum_{j\in\mathcal{N}_i} a_{ij}(\vartheta_{\omega i} - \vartheta_{\omega j}) = k_{\omega i}(\theta_i - \vartheta_{\omega i}). & \text{(38b)} \end{cases}$$

—see Figure 4.

Note that the right-hand side of Eq. (38b) corresponds exactly to that of Eq. (10). Therefore, we know that the dynamic controllers (36), with $\nu_{\omega i} = 0$ reach position consensus. On the other hand, since each of these systems is passive and so is the map (3b) to which it is hinged via the fictitious torsional spring with stiffness $k_{\omega i}$, the vehicles' orientations θ_i are also steered to a consensus manifold $\{\theta_i = \theta_c\}$. This observation stems from an interesting analogy between the control architecture proposed above and (consensus) control of robot manipulators with flexible joints. To better see this, consider the Euler-Lagrange equations for such systems, in closed loop with a proportional-derivative consensus controller like the one defined in (9).

We have—see [7, 58],

$$M_i(\theta_i)\ddot{\theta}_i + C_i(\theta_i,\dot{\theta}_i)\dot{\theta}_i + g_i(\theta_i) = -K(\theta_i - \vartheta_i) \tag{39a}$$

$$\ddot{\vartheta}_i + d_i\dot{\vartheta}_i + p_i \sum_{j\in\mathcal{N}_i} a_{ij}(\vartheta_i - \vartheta_j) = K(\vartheta_i - \theta_i) \tag{39b}$$

and consensus is reached provided that $d_i, p_i > 0$; this follows from the main results in [42].

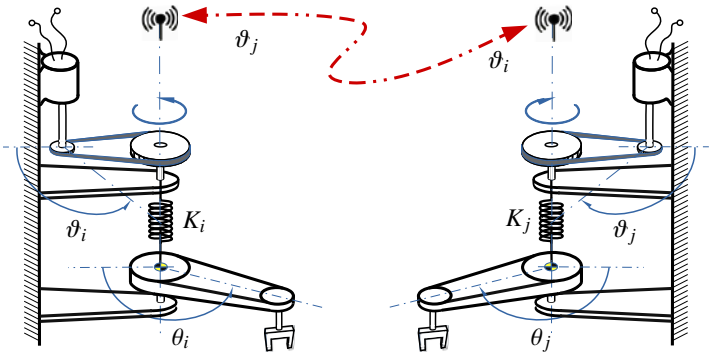

Fig. 5 Schematic representation of a pair of flexible-joint SCARA robots, which move on the plane, unaffected by gravity—compare with the mechanism in the pink block in Figure 4. It is assumed that the robots exchange their actuators measurements ϑ_i over an undirected network. As the actuators reach consensus, so do the arms, in view of their respective mechanical couplings arm-actuator.

In (39), the generalized coordinate ϑ_i corresponds to the actuators' angular position while θ_i corresponds to the links' position. Hence, in the case of the angular motion dynamics, the closed-loop equation $\ddot{\theta}_i = -k_{\omega i}(\theta_i - \vartheta_{\omega i})$ may be assimilated to Eq. (39a) with unitary inertia $M_i = I$ and null Coriolis and gravitational forces, *i.e.,* $C_i = g_i \equiv 0$. On the other hand, the dynamic controller (36) with $\nu_{\omega i} := k_{\omega i}(\theta_i - \vartheta_{\omega i})$ corresponds, up to obvious changes in the notation, to the actuator dynamics in closed loop, that is, Eq. (39b).

Proposition 3 (Output feedback orientation consensus) *Consider the system* (3) *in closed loop with the dynamic controller defined by* (36)*,* (37)*, and* $\nu_{\omega i} := k_{\omega i}(\theta_i - \vartheta_{\omega i})$*. Let Assumption 1 hold. Then, there exist constants* θ_c *and* $\vartheta_c \in \mathbb{R}$ *such that, for all* i *and* $j \leq N$*,*

$$\lim_{t\to\infty} \theta_i(t) = \lim_{t\to\infty} \theta_j(t) = \theta_c, \qquad \lim_{t\to\infty} \omega_i(t) = 0,$$

$$\lim_{t\to\infty} \vartheta_{\omega i}(t) = \lim_{t\to\infty} \vartheta_{\omega j}(t) = \vartheta_c, \qquad \lim_{t\to\infty} \dot{\vartheta}_j(t) = 0.$$

Proof Consider the function

$$W_3(\dot{\vartheta}_\omega, \vartheta_\omega, \theta, \omega) := W_1(\vartheta_\omega, \dot{\vartheta}_\omega) + W_2(\theta, \omega, \vartheta_\omega), \tag{40}$$

where $\vartheta_\omega := [\vartheta_{\omega 1} \cdots \vartheta_{\omega N}]^\top$,

$$W_1(\vartheta_\omega, \dot{\vartheta}_\omega) := \frac{1}{2}\sum_{i\leq N}\Big[\frac{\dot{\vartheta}_{\omega i}^2}{p_{\omega i}} + \frac{1}{2}\sum_{j\in\mathcal{N}_i} a_{ij}(\vartheta_{\omega i} - \vartheta_{\omega j})^2\Big], \tag{41}$$

$$W_2(\theta, \omega, \vartheta) := \frac{1}{2}\sum_{i\leq N}\Big[\frac{\omega_i^2}{p_{\omega i}} + k_{\omega i}(\theta_i - \vartheta_{\omega i})^2\Big]. \tag{42}$$

The function W_2 corresponds to the total energy of the mass-spring (closed-loop) system $\ddot{\theta}_i = -k_{\omega i}(\theta_i - \vartheta_{\omega i})$; the first term is the kinetic energy and the second the potential energy "stored" in the torsional spring of stiffness $k_{\omega i}$. The function W_1 is reminiscent of V_3 in (25). The function W_3 is positive definite in the consensus errors, in ω, ϑ_ω, and $\dot{\vartheta}_\omega$. Moreover, its total derivative along the trajectories of the closed-loop system (38)—with $\dot{\theta}_i = \omega_i$— yields

$$\dot{W}_3(\dot{\vartheta}_\omega, \vartheta_\omega, \theta, \omega) = -\frac{1}{2}\sum_{i\leq N}\frac{d_{\omega i}}{p_{\omega i}}\dot{\vartheta}_{\omega i}^2. \tag{43}$$

Then, the system being autonomous, we may invoke Barbashin-Krasovskĭi's theorem. First, we see that $\dot{W}_3 = 0$ if and only if $\dot{\vartheta}_{\omega i} = 0$. The latter implies that $\ddot{\vartheta}_{\omega i} = 0$ and $\vartheta_{\omega i} = \text{const}$ for all $i \leq N$. From (36) and $\nu_{\omega i} := k_{\omega i}(\theta_i - \vartheta_{\omega i})$ we conclude that $\theta_i = \text{const}$, *i.e.,* $\omega_i = \dot{\omega}_i = 0$. In turn, from $\dot{\omega}_i = -k_{\omega i}(\theta_i - \vartheta_{\omega i}) = -\nu_{\omega i} = 0$ and (36) it follows that

$$\sum_{j\in\mathcal{N}_i} a_{ij}(\vartheta_{\omega i} - \vartheta_{\omega j}) = 0 \quad \text{and} \quad \theta_i = \vartheta_{\omega i}\ \forall\, i, j \leq N.$$

Finally, in view of Assumption 1. The only solution to the equations above is $\theta_i = \vartheta_{\omega i} = \vartheta_c$ for all $i, j \leq N$. □

4.2 Output-feedback position consensus

Akin to the controller for the angular motion subsystem, to steer the Cartesian positions $\bar{z}_i$ to a consensual point on the plane z_c, we use a second-order dynamic controller system that is reminiscent of the equation (8) in closed loop with the control (9), and an added virtual-spring coupling term, $-k_{vi}(\vartheta_{vi} - \bar{z}_i)$. That is, let

$$\ddot{\vartheta}_{vi} + d_{vi}\dot{\vartheta}_{vi} + p_{vi}\sum_{j\in\mathcal{N}_i} a_{ij}(\vartheta_{vi} - \vartheta_{vj}) = -k_{vi}(\vartheta_{vi} - \bar{z}_i), \tag{44}$$

where $\vartheta_{vi} \in \mathbb{R}^2$ and $\dot{\vartheta}_{vi}$ are controller's state variables, and all control gains d_{vi}, p_{vi} and k_{vi} are positive.

Then, the dynamical system (44) is coupled to the double (nonholonomic) integrator (4)—see Figure 4 for an illustration. In contrast to the case of the angular motion, however, for the linear motion the control input u_{vi} must incorporate the change of coordinates defined by φ. Therefore, we define

$$u_{vi} := -\varphi(\theta_i)^\top k_{vi}(\bar{z}_i - \vartheta_{vi}), \quad k_{vi} > 0 \tag{45}$$

—cf. Eq. (37). For the angular-motion dynamics, to overcome the effect of the nonholonomic constraints, the angular-motion control law (37) is endowed with a perturbation term, that is, we define

$$u_{\omega i} := -k_{\omega i}(\theta_i - \vartheta_{\omega i}) + \alpha_i(t, \theta_i, \vartheta_{vi}, \bar{z}_i), \quad k_{\omega i} > 0, \tag{46}$$

The functions α_i are designed to vanish as the control goal is reached. We pose

$$\alpha_i(t, \theta_i, \vartheta_{vi}, \bar{z}_i) := k_{\alpha i}\psi_i(t)\varphi_i(\theta_i)^{\perp\top}(\vartheta_{vi} - \bar{z}_i), \tag{47}$$

which vanishes only as the plant and the controller synchronize, that is, if $\varphi_i(\theta_i)^{\perp\top}(\vartheta_{vi} - \bar{z}_i) \equiv 0$.

Thus, the closed-loop system for the linear-motion dynamics, becomes

$$\Sigma_{vi} : \begin{cases} \dot{\bar{z}}_i = \varphi(\theta_i(t))v_i, & \text{(48a)} \\ \dot{v}_i = -\varphi(\theta_i(t))^\top k_{vi}(\bar{z}_i - \vartheta_{vi}), & \text{(48b)} \\ \ddot{\vartheta}_{vi} + d_{vi}\dot{\vartheta}_{vi} + p_{vi}\sum_{j\in\mathcal{N}_i} a_{ij}(\vartheta_{vi} - \vartheta_{vj}) = -k_{vi}(\vartheta_{vi} - \bar{z}_i); & \text{(48c)} \end{cases}$$

while the closed-loop equations for the angular motion dynamics are modified from (38) into

$$\Sigma_{\omega i} : \begin{cases} \ddot{\theta}_i = -k_{\omega i}(\theta_i - \vartheta_{\omega i}) + \alpha_i(t, \theta_i, \vartheta_{vi}, \bar{z}_i) & \text{(49a)} \\ \ddot{\vartheta}_{\omega i} + d_{\omega i}\dot{\vartheta}_{\omega i} + p_{\omega i}\sum_{j\in\mathcal{N}_i} a_{ij}(\vartheta_{\omega i} - \vartheta_{\omega j}) = k_{\omega i}(\theta_i - \vartheta_{\omega i}). & \text{(49b)} \end{cases}$$

See the blue block in Figure 4 for an illustration.

Note that, as before, in (48) we replaced θ_i with $\theta_i(t)$, which is a valid step as a long as the system is forward complete [23, p. 657]. The latter may be established along similar lines as in Remark 4. Again, the advantage of this is that the overall closed-loop system (38)-(48) may be regarded as a cascaded nonlinear time-varying system as illustrated in Figure 3 (up to a redefinition of α_i). Thus, we have the following [44].

Proposition 4 *(Output-feedback formation consensus) Consider the system* (3)–(5) *in closed loop with* (38b), (46), (47), (45), *and* (44), *with* p_{vi}, d_{vi}, $p_{\omega i}$, *and* $d_{\omega i} > 0$, α_i *as in* (31), ψ_i *and* $\dot{\psi}_i$ *bounded, and* $\dot{\psi}_i$ *persistently exciting. Then, the consensus-formation goal is achieved, that is,* (6) *and* (7) *hold.*

To establish the statement, we use the function

$$\mathcal{V} := \sum_{i \leq N} \left[\frac{1}{p_{vi}} \mathcal{E}_{vi} + \frac{1}{4} \sum_{j \in \mathcal{N}_i} a_{ij} |\vartheta_{vi} - \vartheta_{vj}|^2 \right].$$
$$\mathcal{E}_{vi} := \frac{1}{2} \left[v_i^2 + |\dot{\vartheta}_{vi}|^2 + k_{vi} |\vartheta_{vi} - \bar{z}_i|^2 \right].$$

The function $\mathcal{V}$ is positive definite in the consensus errors $(\vartheta_{vi} - \vartheta_{vj})$ and its derivative yields $\dot{\mathcal{V}} \leq - \sum_{i \leq N} \lambda_{vi} |\dot{\vartheta}_{vi}|^2 \leq 0$. Then, based on the statement and proof of Proposition 3 and arguing as in Remark 4 one may use Barbălat's Lemma to conclude the proof—see [44].

5 Output feedback control under delays

We showed previously how dynamic output-feedback controllers may be successfully designed based on *physical* considerations. Mostly, by designing the controllers as mechanical systems interconnected, on one hand, to the actual plants and, on the other, among themselves in an undirected network. Besides the neat physical interpretation behind, the control method is is versatile, in the sense that one can establish consensus even in the event that the network is affected by time-varying delays.

Technically, the step forward to cover this case, only involves using more sophisticated functions. More precisely, we rely on Lyapunov-Krasovskii functionals. Remarkably, however, the control architecture remains the same as before, so we continue to rely on the certainty-equivalence principle and we use the controllers' dynamics (38b) and (44), except that in the present case, the measurement ϑ_j that the ith vehicle receives from its neighbors is affected by a delay. In that regard, the consensus-error correction terms on the left-hand side of (38b) and (44) depend now on the redefined consensus errors

$$e_{vi} := \sum_{j \in \mathcal{N}_i} a_{ij} \left(\vartheta_{vi} - \vartheta_{vj}(t - T_{ji}(t)) \right), \tag{50}$$

whereas for the orientations,

$$e_{\omega i} := \sum_{j \in \mathcal{N}_i} a_{ij} \left(\vartheta_{\omega i} - \vartheta_{\omega j}(t - T_{ji}(t)) \right). \tag{51}$$

Note that in both cases, as in previous sections, the errors are defined in the controllers' coordinates and not on robots' measured variables.

Based on (45) and (44), the certainty-equivalence controller for the linear motion dynamics, (4), is given by

$$u_{vi} = -k_{vi}\varphi(\theta_i)^\top(\bar{z}_i - \vartheta_{vi}), \tag{52a}$$
$$\ddot{\vartheta}_{vi} = -d_{vi}\dot{\vartheta}_{vi} - k_{vi}(\vartheta_{vi} - \bar{z}_i) - p_{vi}e_{vi}, \tag{52b}$$

whereas, for the angular motion dynamics, we use

$$u_{\omega i} = -k_{\omega i}(\theta_i - \vartheta_{\omega i}) + \alpha_i(t, \theta_i, \vartheta_{vi}, \bar{z}_i), \tag{53a}$$
$$\ddot{\vartheta}_{\omega i} = -d_{\omega i}\dot{\vartheta}_{\omega i} - k_{\omega i}(\vartheta_{\omega i} - \theta_{\omega i}) - p_{\omega i}e_{\omega i}. \tag{53b}$$

All constant parameters are defined as above and α_i is defined in (47), so the controller *per se* remains the same. That is, α_i in (53a) fulfills the same role as explained above. Only the analysis requires more advanced tools. A schematic representation of the networked closed-loop systems is given in Figure 6 below.

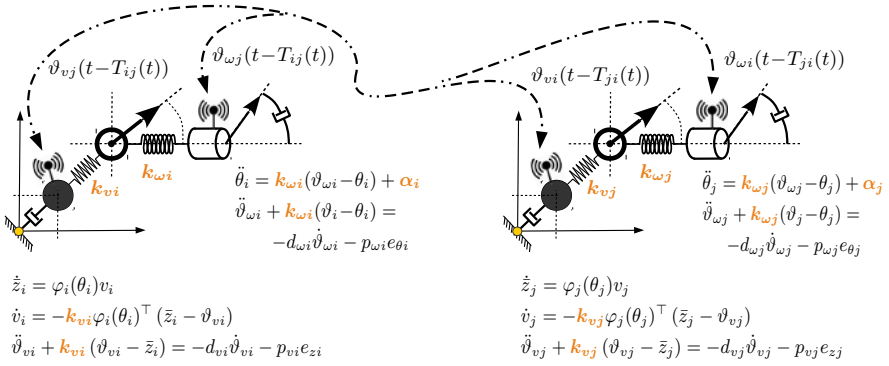

Fig. 6 Schematic representation of two vehicles exchanging their measurements respectively, over a bidirectional limk. On each end, we see the vehicles' linear and angular dynamics coupled with their respective controllers and transmitting the states of the latter over the network. Full consensus of the vehicles is achieved due to the mechanical couplings and the underlying spanning tree in the controllers' network.

Proposition 5 *(Output-feedback consensus under delay measurements) Consider the system* (3)–(5)*, under Assumptions 1–3, in closed loop with* (52)-(53)*. Then, the leaderless consensus control goal is achieved, that is,* (6) *and* (7) *hold provided that*

$$d_{vi} > \frac{1}{2}p_{vi}\sum_{j\in\mathcal{N}_i} a_{ij}\Big[\beta_i + \frac{\overline{T}_{ji}^2}{\beta_j}\Big] \tag{54}$$

$$d_{\omega i} > \frac{1}{2}p_{\omega i}\sum_{j\in\mathcal{N}_i} a_{ij}\Big[\varepsilon_i + \frac{\overline{T}_{ji}^2}{\varepsilon_j}\Big] \tag{55}$$

for some β_i, $\varepsilon_i > 0$*, for all* $i \le N$.

The closed-loop equations, according to the logic of separating the linear and the angular-motion dynamics, correspond to

$$\Sigma_{\omega i}: \begin{cases} \ddot{\theta}_i = -k_{\omega i}(\theta_i - \vartheta_{\omega i}) + \alpha_i(t, \theta_i, \vartheta_{vi}, \bar{z}_i) & \text{(56a)} \\ \ddot{\vartheta}_{\omega i} = -d_{\omega i}\dot{\vartheta}_{\omega i} - k_{\omega i}(\vartheta_{\omega i} - \theta_i) - p_{\omega i}e_{\omega i} & \text{(56b)} \end{cases}$$

$$\Sigma_{vi}: \begin{cases} \dot{\bar{z}}_i = \varphi(\theta_i(t))v_i & \text{(57a)} \\ \dot{v}_i = -k_{vi}\varphi(\theta_i(t))^\top(\bar{z}_i - \vartheta_{vi}) & \text{(57b)} \\ \ddot{\vartheta}_{vi} = -d_{vi}\dot{\vartheta}_{vi} - k_{vi}(\vartheta_{vi} - \bar{z}_i) - p_{vi}e_{vi} & \text{(57c)} \end{cases}$$

The closed-loop system has the same structure as in previous cases. It is a complex network of feedback-interconnected systems and, yet, we can identify in each node of the network a cascaded system as schematically depicted in Figure 3 (up to a redefinition of the arguments of the "perturbation" α_i). That is, for each robot we may replace the state variables θ_i with fixed, but arbitrary, trajectories $\theta_i(t)$ in (57a) and (57b), so the dotted feedback line in Figure 3 is disregarded.

Then, the analysis of $\Sigma_{\omega i}$ and Σ_{vi} may again be carried out using a cascade argument. In a nutshell, one needs to establish that:

(*i*) all the trajectories are bounded: for this we employ the Lyapunov-Krasovskii functional for the "decoupled" linear-motion dynamics (57),

$$\mathcal{V} := \sum_{i\le N}\left[\frac{1}{p_{vi}}\mathcal{E}_i + \frac{1}{4}\sum_{j\in\mathcal{N}_i} a_{ij}|\vartheta_{vi} - \vartheta_{vj}|^2 + \frac{1}{2\beta_i}\Upsilon_i(t,\vartheta_v)\right]$$

$$\mathcal{E}_i := \frac{1}{2}\left[v_i^2 + |\dot{\vartheta}_{vi}|^2 + k_{vi}|\vartheta_{vi} - \bar{z}_i|^2\right]$$

$$\Upsilon_i(t,\vartheta_v) := \sum_{j\in\mathcal{N}_i} a_{ij}\overline{T}_{ij}\int_{-\overline{T}_{ij}}^{0}\int_{t+\eta}^{t}|\dot{\vartheta}_{vj}(\sigma)|^2 d\sigma d\eta.$$

Using the symmetry of the underlying network's Laplacian one can show that

$$\dot{\mathcal{V}} \le -\sum_{i\le N}\left[\frac{d_{vi}}{p_{vi}} - c(\overline{T}_{ij})\right]|\dot{\vartheta}_{vi}|^2. \tag{58}$$

Hence, under the assumption that (54) holds, we have $\dot{\mathcal{V}} \le 0$ which implies that the consensus errors $\vartheta_{vi} - \vartheta_{vj}$ as well as v_i and $\dot{\vartheta}_{vi}$ are bounded (at least on the interval of existence of the solutions—see Remark 4).

On the other hand,

(*ii*) for $\Sigma_{\omega i}$ with $\alpha_i \equiv 0$ we may use the Lyapunov-Krasovskii functional

$$\mathcal{W} := \sum_{i\le N}\left[\frac{1}{p_{\omega i}}\mathcal{H}_i + \frac{1}{4}\sum_{j\in\mathcal{N}_i} a_{ij}(\vartheta_{\omega i} - \vartheta_{\omega j})^2 + \frac{1}{2\varepsilon_i}\Upsilon_i(t,\vartheta_\omega)\right]$$

$$\mathcal{H}_i := \frac{1}{2}\left[\omega_i^2 + \dot{\vartheta}_{\omega i}^2 + k_{\omega i}(\vartheta_{\omega i} - \theta_i)^2\right]$$

$$\Upsilon_i(t, \vartheta_\omega) := \sum_{j \in \mathcal{N}_i} a_{ij}\overline{T}_{ij} \int_{-\overline{T}_{ij}}^{0} \int_{t+\eta}^{t} |\dot{\vartheta}_{\omega j}(\sigma)|^2 d\sigma d\eta$$

to obtain that

$$\dot{\mathcal{W}} \leq -\sum_{i \leq N}\left[\frac{d_{\omega i}}{p_{\omega i}} - c(\overline{T}_{ij})\right]\dot{\vartheta}_{\omega_i}^2. \tag{59}$$

Again, under condition (55) we have $\dot{\mathcal{W}} \leq 0$, from which one conclude the boundedness of the orientation consensus errors, as well as of the angular velocities ω_i.

From here, one may carry on using recursively Barbălat's Lemma and the boundedness of α_i to establish the convergence of multiple signals. Finally,

(*iii*) under the persistently exciting effect of α_i, one ensures that the trajectories can only converge to the consensus manifold, thereby avoiding the undesired equilibria discussed in Section 3.2.

The detailed proof is available from [45].

6 An illustrative case-study

We used the simulator Gazebo-ROS and the Robot Operating System (ROS) interface to evaluate the performance of our controller in a scenario that reproduces as closely as possible that of a laboratory experimental benchmark. Furthermore, for the sake of comparison, we also carried out numerical-integration simulations using Simulink of Matlab.

Gazebo-ROS is an efficient 3D dynamic simulator of robotic systems in indoor and outdoor environments. In contrast to pure numerical-integration based solvers of differential equations, Gazebo-ROS accurately emulates physical phenomena and dynamics otherwise neglected, such as friction, contact forces, actuator dynamics, slipping, *etc.* In addition, it offers high-fidelity robot and sensor simulations.

For the test scenario we employed the model of a PIONEER 3-DX wheeled robot [16], available in Gazebo's library. It must be underlined that for this robot the center of mass is not located on the axis joining the two wheels' centers –cf. Figure 1, as it is assumed at the basis of the developments in the previous sections. More precisely, in Equations (2) the functions F_v and F_ω include Coriolis terms that are quadratic in the velocities, *i.e.,* $\frac{r_i}{3}\omega_i^2$ on the left-hand side of Equation (2a) and $-\frac{r_i m_i}{3I_i}\omega_i v_i$ on the left-hand side of Equation (2b). Akin to an actual experimentation set-up, these constitute dynamic effects not considered in the model for which the controller is validated analytically, nor in the simulations carried out with Simulink of Matlab.

Concretely, in the simulation scenario we consider six PIONEER 3D-X robots starting from initial postures as defined in the 2nd-4th columns of Table 1, below.

Also, an illustration of the robots in their initial postures is showed via a screenshot of the Gazebo-ROS simulator's user interface in Figure 7, below.

Table 1 Initial conditions and formation offsets

Index	x_i [m]	y_i [m]	θ_i [rad]	δ_{xi} [m]	δ_{yi} [m]
1	8	7	1.57	2	0
2	2	13	0.0	1	2
3	2	9	-0.39	-1	2
4	-2	6	0.39	-2	0
5	1	3	-0.39	-1	-2
6	4	4	-0.39	1	-2

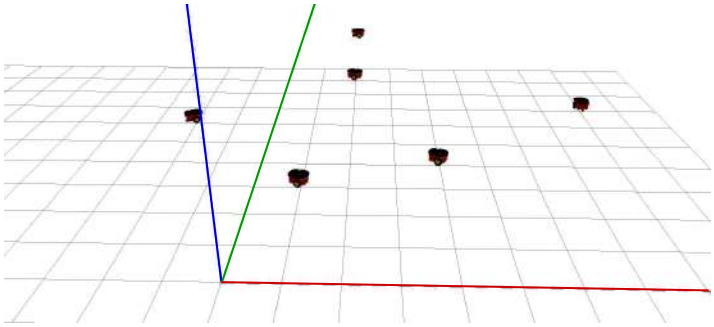

Fig. 7 Screenshot of the six PIONEER 3D-X robots' at their initial configuration, in the Gazebo-ROS simulator

It is assumed that the robots communicate over the undirected connected graph like the one illustrated in Figure 8 and with piece-wise constant time-varying delays. For simplicity, all the time delays $T_{ji}(t)$ are taken equal; they are generated randomly following a normal distribution with mean $\mu = 0.3$, variance $\sigma^2 = 0.0003$ and a sample time of 10 ms —see Figure 9. Such time delay (non-smooth but piece-wise continuous) does not satisfy Assumption 2 since its time-derivative is bounded only almost everywhere (that is, except at the points of discontinuity). However, it is considered in the simulations since it is closer to what is encountered in a real-world set-up [1]. Even though the technical Assumption 2 does not hold, full consensus is achieved (at least practically) in both the Matlab and the realistic Gazebo-ROS simulations. This hints at the fact that Assumption 2 might be relaxed in the analysis, albeit using a different controller —cf. [33].

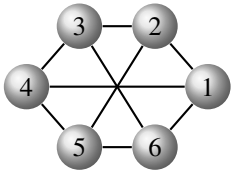

Fig. 8 Communication topology: undirected connected graph

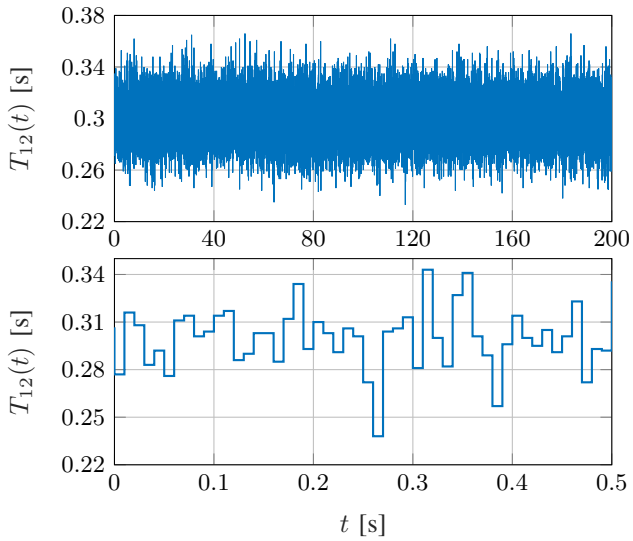

Fig. 9 Variable delay between the robot 1 and the received information from neighbor 2.

The desired formation at rendezvous corresponds to a hexagon determined by desired offsets $\delta_i = (\delta_{xi}, \delta_{yi})$ with respect the unknown center of the formation. These constants are presented in the last two columns of Table 1 —see Figure 2 for an illustration of the target formation.

For a fair and meaningful comparison, the numerical simulations under Simulink of Matlab were performed using the information available on the PIONEER 3D-X robot, from the Gazebo-ROS simulator. For simplicity, it is assumed that all the robots have the same inertial and geometrical parameters given by $m = 5.64$ kg, $I = 3.115$ kg·m^2, $r = 0.09$ m and $R = 0.157$ m.

In both simulators, the control gains were set to $k_{vi} = 1$, $k_{\omega i} = 2$, $d_{vi} = 3$, $p_{vi} = 0.4$, $d_{\omega i} = 2$, $p_{\omega i} = 0.1$, for all $i \in [1, 6]$. These values correspond to magnitudes compatible with the emulated physics of the PIONEER 3D-X robots in Gazebo-ROS and are chosen so that the poles of the 2nd-order system $\ddot{x} = -d_{(\cdot)}\dot{x} - p_{(\cdot)}x$ have negative real parts and the system have an over-damped step-response. The δ-persistently-exciting functions α_i, for all $i \in [1, 6]$, were taken as in (53) with $k_{\alpha i} = 0.4$ and, for simplicity, (multi)periodic functions

$$\begin{aligned} \psi_i(t) \;=\; & 2.5 + \sin(2\pi t) + 0.3\cos(6\pi t) - 0.5\sin(8\pi t) \\ & -0.1\cos(10\pi t) + \sin(\pi t) \quad \forall\, i \leq 6. \end{aligned} \tag{60}$$

Other parameters such as the sampling time, were taken equal.

As we mentioned above, however, certain physical phenomena as well as actuator and sensor dynamics, which are hard-coded in Gazebo-ROS, cannot be reproduced in Matlab. The consequence of this is clearly appreciated in the figures showed below.

The results obtained with Gazebo-ROS are showed in Figs. 11, 13, 15, and 17. Those obtained using Simulink™ of Matlab™ are showed in Figs. 10, 14, 16, and 18.

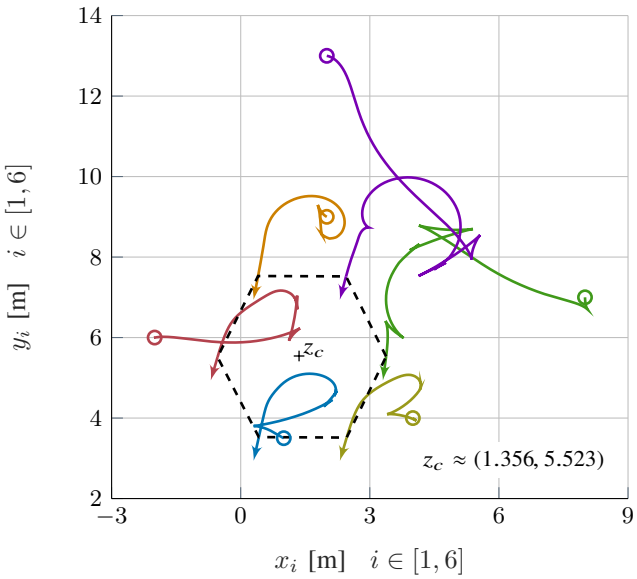

Fig. 10 Paths followed by the PIONEER 3D-X robots up to full formation consensus—Matlab simulation. A hexagonal formation is achieved with coinciding orientations (illustrated by arrows).

In both cases the robots appear to achieve consensus, *i.e.,* to meet at a non-predefined rendezvous point in hexagonal formation and with common non-predefined orientation—see Figs. 10 and 11, as well as the screenshot of the final postures from Gazebo's graphical interface, Figure 12. Under Matlab, the center of the formation is located at $(1.356, 5.523)$, while under Gazebo-ROS it is at $(-3.242, -3.597)$. The consensual orientations are $\theta_c \approx -2.889$ rad under Gazebo-ROS and $\theta_c \approx -1.785$ rad under Matlab.

Both simulations illustrate that for networks of nonholonomic vehicles, the initial conditions do not determine the consensus point, as is the case of linear systems interconnected over static undirected connected graphs [52]. Indeed, the consensus point—in this case the center of the formation and the common orientation—does not correspond to the average of the initial conditions.

The consensus equilibrium heavily depends, as well, on the systems' *nonlinear* dynamics. This is clear both, in Figure 10 which results of a Matlab simulation for a network of nonlinear systems modeled as in (1)-(2) with $F_v = F_\omega = 0$, as well as in Figure 11 which results from a more realistic simulation based on a model that emulates otherwise neglected Coriolis high-order terms, friction, sensor and actuator effects, *etc.* In addition, it appears fitting to recall that the controller, in both cases, is dynamic and time-varying.

Furthermore, it is clear from Figs. 10 and 11 that the results obtained with either simulator differ considerably in various manners. Obvious discrepancies lay in the position of the center of the consensus formation that is achieved, as well as in the paths followed by the robots.

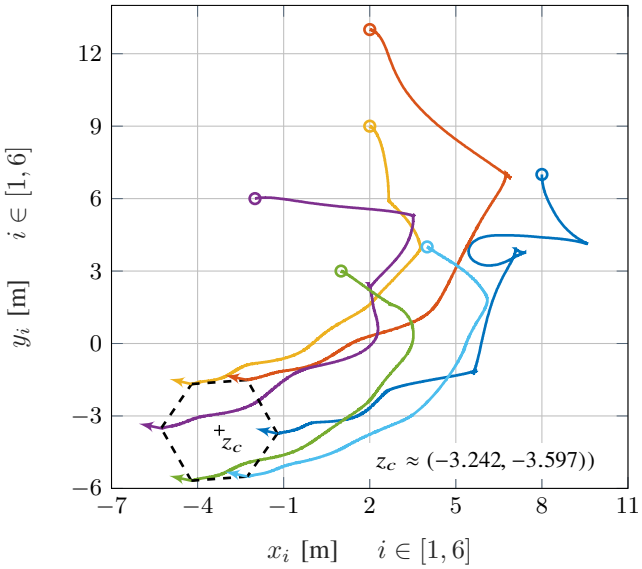

Fig. 11 Paths followed by the PIONEER 3D-X robots up to full formation consensus—Gazebo-ROS simulation. A hexagonal formation is achieved with coinciding orientations (illustrated by arrows).

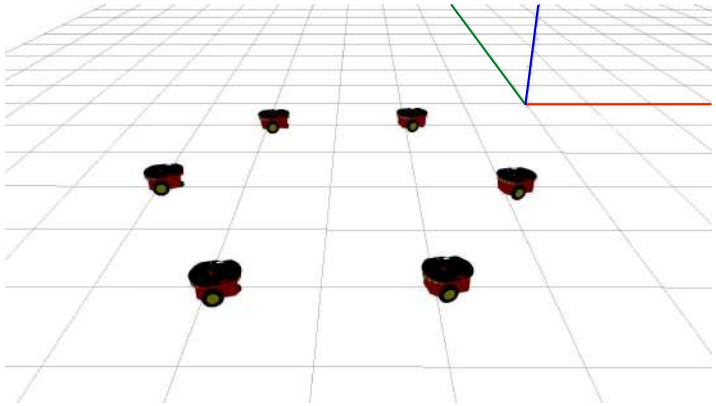

Fig. 12 Screenshot of the final configuration in the Gazebo-ROS simulator; the six robots achieving full consensus at the rendezvous point.

The differences in the transient behaviors for both simulations are even clearer in the plots of the consensus errors, which, for the purpose of graphic illustration, are defined as the difference between each robot's variables and the corresponding average:

$$e_{zi} := \bar{z}_i - \frac{1}{N}\sum_{j\in\mathcal{N}_i} \bar{z}_j, \quad e_{\theta i} := \theta_i - \frac{1}{N}\sum_{j\in\mathcal{N}_i} \theta_j. \tag{61}$$

That is, the limits in (6) and (7) hold if the error trajectories $e_{zi}(t)$ and $e_{\theta i}(t)$ as defined above converge to zero, but the errors in (61) do not correspond to variables actually used by the controller nor measured for that matter.

In Figure 13 one can appreciate that such errors do not actually tend to zero, but to a steady state-error—a keen observer will notice that the hexagon in Figure 11 is actually not quite so. In contrast to this, in the simulation obtained using Matlab—see Figure 14— the errors converge to zero asymptotically, albeit slowly. The reason is that in the Gazebo-ROS simulation, after a transient, the amplitude of the input torques becomes considerably small in absolute value—see Figure 17.

The presence of a steady-state error and the persistency-of-excitation effect in the controller maintain the input torques oscillating (periodically in this case due to the choice of $\psi_i(t)$ in (60)), but, *physically*, they result insufficient to overcome the robots' inertia and friction forces that oppose their forward and angular motions. In contrast to this, in Figure 18 are showed the input torques obtained using Simulink of Matlab. A similar oscillating behavior is observed, but the torques vanish asymptotically—notice the order of magnitude in the plots on the right column in Figure 18, in the range of milli-Nm— as the error-dependent persistency of excitation disappears.

It seems fitting to say at this point that the controller gains may be augmented, for instance, to increase the convergence speed, but such values may result incompatible with the robots' and actuators' physical limitations, so it is not done here to conserve a realistic setting.

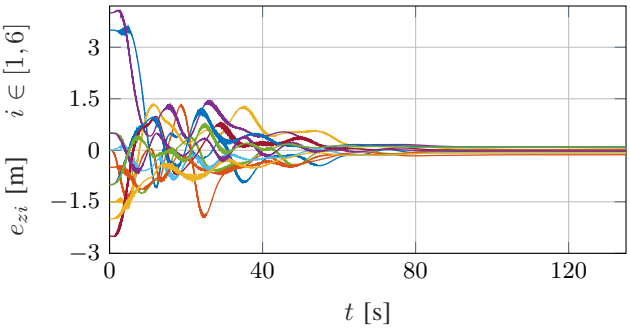

Fig. 13 Position consensus errors—Gazebo-ROS simulation.

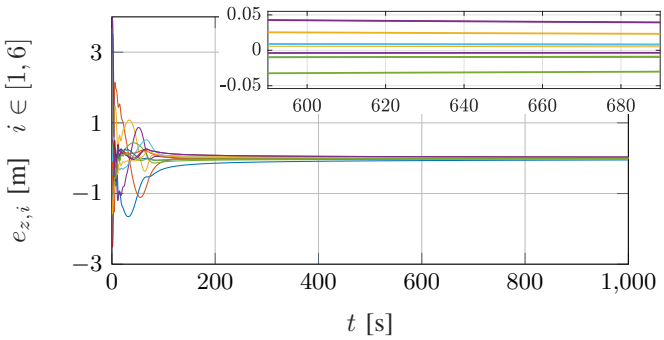

Fig. 14 Position consensus errors—Matlab simulation.

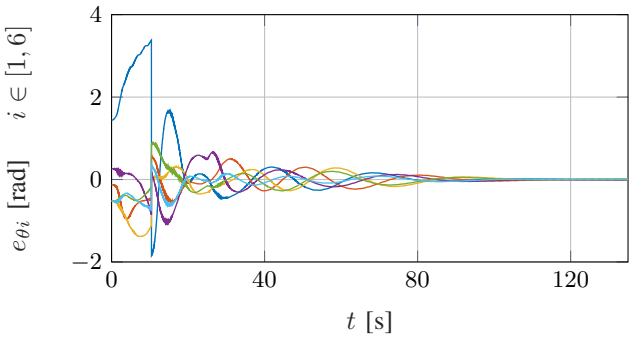

Fig. 15 Orientation consensus errors—Gazebo-ROS simulation. The consensus equilibrium $\theta_c \approx -2.889$ rad.

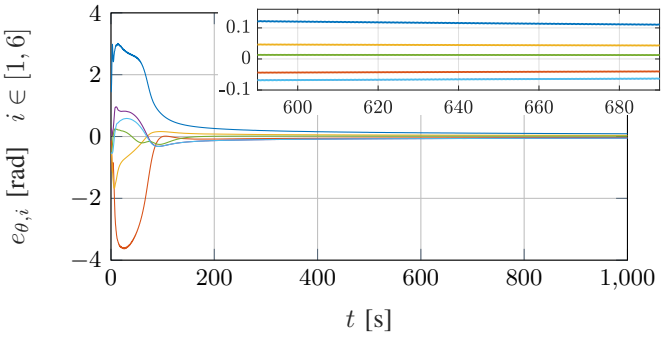

Fig. 16 Orientation consensus errors—Matlab simulation. The consensus equilibrium $\theta_c \approx -1.785$ rad

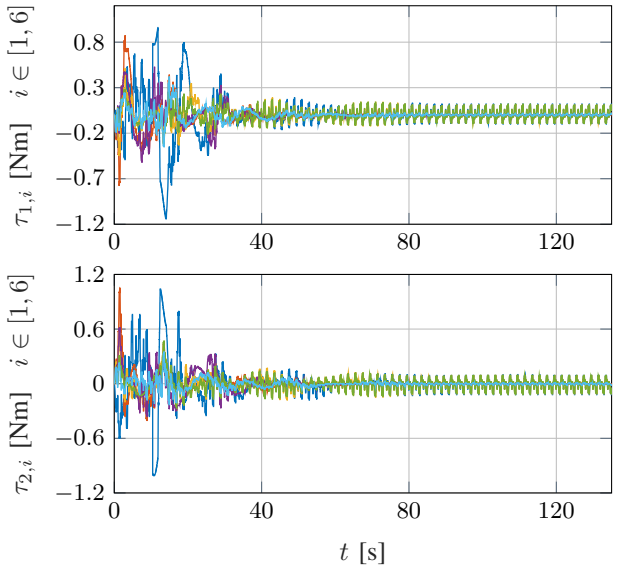

Fig. 17 Input torques—Gazebo-ROS simulation.

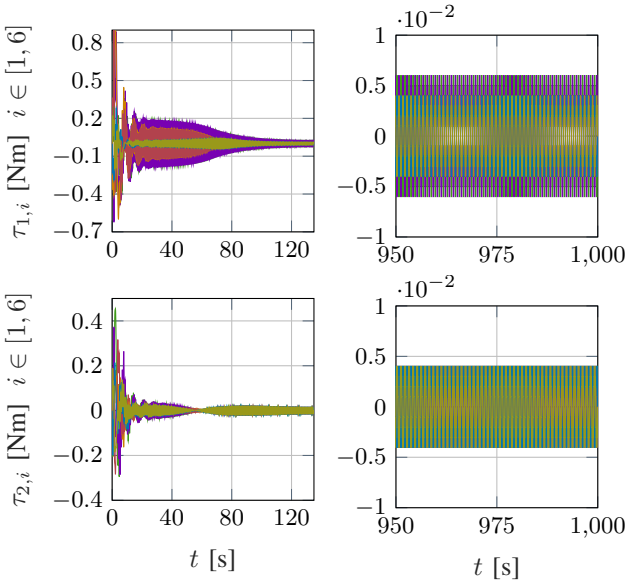

Fig. 18 Input torques—Matlab simulation.

7 Conclusions

We described a simple and appealing control method for formation-consensus of differential-drive robots that applies in realistic scenarii including those of vehicles non-equipped with velocity sensors and networks affected by time-varying delays. The controllers that we propose have the neat physical interpretation of a second order mechanical system itself, so this technique may be a starting point for observer-less control of multi-agent systems under output feedback. It appears interesting to continue testing the limits of our physics-based method for output feeback control in a multi-agent systems setting.

Notably, our hypothesis that the graph is undirected and static remains conservative, but the study of multi-agent nonholonomic vehicles with less stringent hypotheses on the topology has been little addressed, even under the assumption that full-state feedback is available. It has certainly been done for second-order integrators, as in [51], for directed-spanning-tree-graph topologies or for high-order systems under constraints in [54], but the *consensus* control of nonholonomic systems networked over generic directed graphs and under output feedback remains very little explored. A major stumbling block remains the construction of strict Lyapunov functions to establish ISS when the graph is directed and admits cycles (hence, beyond leader-follower configurations). Although the problem was recently solved for linear systems in [49], to the best of our knowledge, it remains largely open for nonholonomic systems.

Another intriguing aspect to investigate further is the influence of the nonlinear dynamics on consensus. Our numerical tests using the Gazebo-ROS simulator clearly show the effects of the nonlinearities in the consensus and the limitations of numerical algorithms bound to solving ordinary differential equations that describe over-simplified models, in which aspects such as unmodelled dynamics, friction and, actuator and sensor dynamics are neglected. It is important to study formally the consensus-formation control problems using models that include the presence of highly nonlinear Lagrangian dynamics—*cf.* [24, 13, 19, 59].

References

1. A. Abdessameud, I.G. Polushin, and A. Tayebi. Synchronization of Lagrangian systems with irregular communication delays. *IEEE Trans. Autom. Control*, 59(1):187–193, 2014.
2. A. Abdessameud, A. Tayebi, and I. G. Polushin. Leader-follower synchronization of euler-lagrange systems with time-varying leader trajectory and constrained discrete-time communication. *IEEE Trans. Autom. Control*, 62(5):2539–2545, May 2017.
3. Abdelkader Abdessameud and Abdelhamid Tayebi. On consensus algorithms for double-integrator dynamics without velocity measurements and with input constraints. *Syst. Control Lett.*, 59(12):812–821, 2010.
4. E. A. Barbashin and N. N. Krasovskiĭ. Об устойчивости движения в целом. *Dokl. Akad. Nauk. USSR*, 86(3):453–456, 1952. Commonly (and wrongly) cited in English under: "On the stability of motion in the large"; Correct translation: "On the stability of motion in the *whole*".

5. A. Bautista-Castillo, C. Lopez-Franco, and E. Nuño. Consensus-based formation control for multiple nonholonomic robots. In *2016 IEEE Int. Autumn Meet. Power Elec. Comp. (ROPEC)*. IEEE, 2016.
6. R. W. Brockett. Asymptotic stability and feedback stabilization. *Differential geometric control theory*, 27(1):181–191, 1983.
7. I. V. Burkov and A. T. Zaremba. Dynamics of elastic manipulators with electric drives. *Izv. Akad. Nauk SSSR Mekh. Tverd. Tela*, 22(1):57–64, 1987. Engl. transl. in Mechanics of Solids, Allerton Press.
8. Y. Cao and W. Ren. *Distributed Coordination of Multi-agent Networks: Emergent Problems, Models, and Issues*. Springer-Verlag, 2011.
9. Y. Cheng, R. Jia, H. Du, G. Wen, and W. Zhu. Robust finite-time consensus formation control for multiple nonholonomic wheeled mobile robots via output feedback. *Int. J. Robust Nonlinear Control*, 28(6):2082–2096, 2018.
10. L. Consolini, F. Morbidi, D. Prattichizzo, and M. Tosques. On a class of hierarchical formations of unicycles and their internal dynamics. *IEEE Trans. Autom. Control*, 57(4):845–859, 2012.
11. D.V. Dimarogonas and K.J. Kyriakopoulos. On the rendezvous problem for multiple nonholonomic agents. *IEEE Trans. Autom. Control*, 52(5):916–922, May 2007.
12. W. E. Dixon, D. M. Dawson, F. Zhang, and E. Zergeroglu. Global exponential tracking control of a mobile robot system via a PE condition. *IEEE Trans. Systems, Man, and Cybernetics B*, 30(1):129–142, 2000.
13. K. D. Do, Z.-P. Jiang, and J. Pan. A global output-feedback controller for simultaneous tracking and stabilization of unicycle-type mobile robots. *IEEE Trans. Robot. Autom.*, 20(3):589–594, 2004.
14. W. Dong. Distributed observer-based cooperative control of multiple nonholonomic mobile agents. *Int. J. Syst. Sc.*, 43(5):797–808, 2012.
15. M. I. El-Hawwary and M. Maggiore. Distributed circular formation stabilization for dynamic unicycles. *IEEE Trans. Autom. Control*, 58(1):149–162, 2013.
16. Génération Robots. Pioneer P3-DX mobile robot. Accessed May 06, 2021. [Online]. https://www.generationrobots.com/en/402395-robot-mobile-pioneer-3-dx.html.
17. A. González, R. Aragüés, G. López-Nicolás, and C. Sagüés. Stability analysis of nonholonomic multiagent coordinate-free formation control subject to communication delays. *Int. J. Robust Nonlinear Control*, 28(14):4121–4138, 2018.
18. A. T. Hernández, A. Loría, E. Nuño, and E. Panteley. Consensus-formation control of nonholonomic robots without velocity measurements. In *Proc. European Control Conf.*, pages 674–679, St. Petersburg, Russia, 2020.
19. J. Huang, C. Wen, W. Wang, and Z.-P. Jiang. Adaptive output feedback tracking control of a nonholonomic mobile robot. *Automatica*, 50:821–831, 2014.
20. Q. Hui. Finite-time rendezvous algorithms for mobile autonomous agents. *IEEE Trans. Autom. Control*, 56(1):207–211, 2011.
21. A. Jadbabaie, J. Lin, and A. S. Morse. Coordination of groups of mobile autonomous agents using nearest neighbor rules. *IEEE Trans. Autom. Control*, 48(6):988–1001, 2003.
22. J. Jin and N. Gans. Collision-free formation and heading consensus of nonholonomic robots as a pose regulation problem. *Robot. Autonomous Syst.*, 95(9):25–36, 2017.
23. H. Khalil. *Nonlinear systems*. Macmillan Publishing Co., 2nd ed., New York, 1996.
24. D. Lee. Passive decomposition and control of nonholonomic mechanical systems. *IEEE Trans. Robot.*, 26(6):978–992, 2010.
25. T. C. Lee, Kai. T. Song, C. H. Lee, and C. C. Teng. Tracking control of unicycle-modeled mobile robots using a saturation feedback controller. *IEEE Trans. Control Syst. Technol.*, 9(2):305–318, 2001.
26. Z. Li, W. Ren, X. Liu, and M. Fu. Consensus of multi-agent systems with general linear and lipschitz nonlinear dynamics using distributed adaptive protocols. *IEEE Trans. Autom. Control*, 58(7):1786–1791, 2013.
27. X. Liang, H. Wang, Y. Liu, W. Chen, and T. Liu. Formation control of nonholonomic mobile robots without position and velocity measurements. *IEEE Trans. Robot.*, 34(2):434–446, 2018.

28. Z. Lin, B. Francis, and M. Maggiore. Necessary and sufficient graphical conditions for formation control of unicycles. *IEEE Trans. Autom. Control*, 50(1):121–127, 2005.
29. D. A. Lizárraga. Obstructions to the existence of universal stabilizers for smooth control systems. *Math. Control, Sign. Syst.*, 16:255–277, 2004.
30. A. Loría. From feedback to cascade-interconnected systems: Breaking the loop. In *Proc. 47th. IEEE Conf. Decis. Contr.*, pages 4109–4114, Cancun, Mex., 2008.
31. A. Loría, E. Panteley, and A. Teel. A new persistency-of-excitation condition for UGAS of NLTV systems: Application to stabilization of nonholonomic systems. In *Proc. 5th. European Contr. Conf.*, pages 1363–1368, Karlsrühe, Germany, 1999.
32. M. Maghenem. *Stability and stabilization of networked time-varying systems*. PhD thesis, Univ Paris Saclay, Gif sur Yvette, 2017. https://tel.archives-ouvertes.fr/tel-01596158.
33. M. Maghenem, A. Loría, E. Nuño, and E. Panteley. Distributed full-consensus control of nonholonomic vehicles under non-differentiable measurement delays. *IEEE Control Syst. Lett.*, 5(1):97–102, 2021.
34. W. Mao, C. Wang, W. Chen, and X. Li. Observer-based consensus design for multi-agent systems with unavailable velocities of leader and followers. In *Proc. 32nd Chinese Control Conf.*, pages 7030–7033, 2013.
35. J. A. Marshall, M. E. Broucke, and B. A. Francis. Formations of vehicles in cyclic pursuit. *IEEE Trans. Autom. Control*, 49(11):1963–1974, 2004.
36. E. Montijano, J. Thunberg, X. Hu, and C. Sagüés. Epipolar visual servoing for multirobot distributed consensus. *IEEE Trans. Robot.*, 29(5):1212–1225, 2013.
37. N. Moshtagh and A. Jadbabaie. Distributed geodesic control laws for flocking of nonholonomic agents. *IEEE Trans. Autom. Control*, 52(4):681–686, 2007.
38. K. S. Narendra and A. M. Annaswamy. *Stable adaptive systems*. Prentice-Hall, Inc., New Jersey, 1989.
39. J. I. Neimark and F. A. Fufaev. *Dynamics of Nonholonomic Systems*, volume 33. A.M.S. Translations of Mathematical Monographs, Providence, RI, 1972.
40. B. Ning and Q. Han. Prescribed finite-time consensus tracking for multiagent systems with nonholonomic chained-form dynamics. *IEEE Trans. Autom. Control*, 64(4):1686–1693, 2019.
41. E. Nuño. Consensus of Euler-Lagrange systems using only position measurements. *IEEE Trans. Control Netwk. Syst.*, 5(1):489–498, 2018.
42. E. Nuño and R. Ortega. Achieving consensus of Euler-Lagrange agents with interconnecting delays and without velocity measurements via passivity-based control. *IEEE Trans. Control Syst. Technol.*, 26(1):222–232, 2018.
43. E. Nuño, A. Loría, A. T. Hernández, M. Maghenem, and E. Panteley. Distributed consensus-formation of force-controlled nonholonomic robots with time-varying delays. *Automatica*, (120):109114, 2020.
44. E. Nuño, A. Loría, and E. Panteley. Leaderless consensus formation control of cooperative multi-agent vehicles without velocity measurements. *IEEE Control Systems Letters*, 6:902–907, 2022.
45. E. Nuño, A. Loría, E. Panteley, and E. Restrepo-Ochoa. Rendezvous of nonholonomic robots via output-feedback control under time-varying delays. *IEEE Trans. Contr. Syst. Technol.*, 30(6):2707–2716, 2022.
46. E. Nuño, I. Sarras, A. Loría, M. Maghenem, E. Cruz-Zavala, and E. Panteley. Strict Lyapunov-Krasovskii functionals for undirected networks of Euler-Lagrange systems with time-varying delays. *Syst. & Contr. Letters*, 135:104579, Jan 2020.
47. E. Panteley, E. Lefeber, A. Loría, and H. Nijmeijer. Exponential tracking of a mobile car using a cascaded approach. In *IFAC Workshop on Motion Control*, pages 221–226, Grenoble, France, 1998.
48. E. Panteley and A. Loría. Synchronization and dynamic consensus of heterogeneous networked systems. *IEEE Trans. Autom. Control*, 62(8):3758–3773, 2017.
49. E. Panteley, A. Loría, and S. Sukumar. Strict lyapunov functions for consensus under directed connected graphs. In *Proc. European Control Conference (ECC)*, pages 935–940, St. Petersburg, Russia, 2020.

50. H. A. Poonawala, A. C. Satici, and M. W. Spong. Leader-follower formation control of nonholonomic wheeled mobile robots using only position measurements. In *Proc. 9th Asian Control Conf.*, pages 1–6, 2013.
51. H. A. Poonawala and M. W. Spong. Preserving strong connectivity in directed proximity graphs. *IEEE Trans. Autom. Control*, 62(9):4392–4404, 2017.
52. W. Ren and R. W. Beard. *Distributed consensus in multivehicle cooperative control*. Springer verlag, 2005.
53. E. Restrepo, A. Loría, I. Sarras, and J. Marzat. Stability and robustness of edge-agreement-based consensus protocols for undirected proximity graphs. *Int. J. of Control*, 2020.
54. E. Restrepo-Ochoa, A. Loría, I. Sarras, and J. Marzat. Robust consensus of high-order systems under output constraints: Application to rendezvous of underactuated UAVs. *IEEE Trans. on Automatic Control*, 68(1):329–342, 2023.
55. Ashton Roza, Manfredi Maggiore, and Luca Scardovi. A Smooth Distributed Feedback for Global Rendezvous of Unicycles. *IEEE Trans. Control Netw. Syst.*, 5(1):640–652, March 2018.
56. C. Samson. Time-varying stabilization of a car-like mobile robot. Technical report, INRIA Sophia-Antipolis, 1990. In *Proc. in advanced robot control* **162** (Springer, Berlin, 1991).
57. C. Samson. Control of chained system: Application to path following and time-varying point stabilization of mobile robots. *IEEE Trans. Autom. Control*, 40(1):64–77, 1995.
58. M. Spong. Modeling and control of elastic joint robots. *ASME J. Dyn. Syst. Meas. Contr.*, 109:310–319, 1987.
59. S. G. Tzafestas. *Introduction to mobile robot control*. Elsevier Inc, First ed., 2013.
60. P. Wang and B. Ding. Distributed RHC for tracking and formation of nonholonomic multi-vehicle systems. *IEEE Trans. Autom. Control*, 59(6):1439–1453, 2014.
61. X. Wang and Y. Hong. Distributed observers for tracking a moving target by cooperative multiple agents with time delays. In *2009 ICCAS-SICE*, pages 982–987, 2009.
62. C. Yang, W. Xie, C. Lei, and B. Ma. Smooth time-varying formation control of multiple nonholonomic agents. In *Proc. Chinese Intel. Syst. Conf.*, pages 283–291. Springer, 2016.
63. S. Zhao. Affine formation maneuver control of multiagent systems. *IEEE Trans. Autom. Control*, 63(12):4140–4155, 2018.
64. X. Zhao, X. Zheng, C. Ma, and R. Li. Distributed consensus of multiple Euler-Lagrange systems networked by sampled-data information with transmission delays and data packet dropouts. *IEEE Trans. Autom. Sc. Engg.*, 14(3):1440–1450, 2017.